Inorg. Chem. **2003**, *42*, 4232–4240

Intercalation of $[Cr(C_2O_4)_3]^{3-}$ Complex in Mg,Al Layered Double Hydroxides

M. del Arco, S. Gutiérrez, C. Martín, and V. Rives*

Departamento de Química Inorgánica, Universidad de Salamanca, Salamanca, 37008 Spain

Received January 14, 2003

A Mg,Al layered double hydroxide (LDH) with $[Cr(C_2O_4)_3]^{3-}$ anions in the interlayer has been synthesized following two different routes: reconstruction from a mildly calcined Mg,Al-carbonate LDH, and anion exchange from a Mg,Al-nitrate LDH. The solids prepared have been characterized by elemental chemical analysis, powder X-ray diffraction, FT-IR and UV–vis/DR (diffuse reflectance) spectroscopies, thermal methods, nitrogen adsorption at –196 °C, and FT-IR monitoring of pyridine adsorption. The results obtained indicate that the most appropriate method is anion exchange, leading to a well crystallized LDH with an interlayer spacing of 10 Å. Due to the high pH value (>8) of the solution in the reconstruction method, however, a polyphasic system is obtained, where, in addition to a phase with the LDH structure, amorphous magnesium oxalate and chromium oxohydroxides are also formed due to hydrolysis of the complex. The interlayer complex is stable up to 200 °C, but the layered structure is stable up to 330 °C, probably because of the presence of interlayer oxalate anions formed during decomposition of the complex. Calcination leads to oxidation of Cr^{3+} ions to the six-valent state, which reverts to Cr^{3+} when the calcination temperature is further increased.

Introduction

Layered double hydroxides (LDHs), also known as anionic clays, are layered compounds whose structure can be considered as derived from brucite, $Mg(OH)_2$, where some M^{II}/M^{III} substitution has taken place, electric balance being attained through intercalation of anions between the interlayers, where water molecules are also present. These solids, also known as hydrotalcites, because of the mineral with this structure and the formula $Mg_6Al_2(OH)_{16}CO_3 \cdot 4H_2O$, have attracted much attention because of their applications as catalysts, catalyst precursors, anion exchangers, adsorbents, etc.[1−3] The general formula can be written as $[M_{1-x}^{II}M_x^{III}(OH)_2]A^{m-}_{x/m} \cdot nH_2O$, or shortened as M^{II},M^{III}—A. Many synthetic LDHs can be prepared by different combinations of M^{II}, M^{III}, and A^{m-} components.[4,5] As A^{m-} can be exchanged, these compounds are themselves precursors for a large number of new LDHs. Anions can be simple ones, as carbonate, nitrate, chloride, etc., or bulk anions, such as polyoxometalates or even Keggin, Finke, or Dawson-type anions. The height of the interlayer space depends both on the nature of the anion and on its orientation, if it is not spherical.[6−8] Intercalation of these anions can be achieved following different methods, and in some cases, preswelling of the layers is required.[9,10]

Recent reviews[11,12] have demonstrated that, despite the well-known stability of oxalate complexes (stable in a wide pH range), very few papers deal with the study of LDHs with intercalated oxalate complexes. Moreover, the complexation properties of the oxalic acid and its anion oxalate toward metal cations are used in the so-called oxalate

* To whom all correspondence should be addressed. E-mail: vrives@usal.es. Fax: +34 923 29 45 74.

(1) Cavani, F.; Trifiró, F.; Vaccari, A. *Catal. Today* **1991**, *11*, 1.
(2) Trifiró, F.; Vaccari, A. In *Comprehensive Supramolecular Chemistry*; Atwood, J. L., Davis, J. E. D., MacNicol, D. D., Vogtle, F., Lehn, J. M., Alberti, G., Bein, T., Eds.; Pergamon-Elsevier Science Ltd.: Oxford, U.K., 1996.
(3) de Roy, A.; Forano, C.; El Malki, K.; Besse, J. P. In *Expanded Clays and other Microporous Solids*; Occelli, M. L., Robson, H. E., Eds.; Van Nostrand Reinhold: New York, 1992.
(4) Reichle, W. T. *Solid State Ionics* **1986**, *22*, 135.
(5) Corrado, K. A.; Kostapapas, A.; Suib, S. L. *Solid State Ionics* **1988**, *26*, 77.
(6) Drezdzon, M. A. *ACS Symp. Ser*. **1990**, *437*, 140.
(7) Clearfield, A.; Kuchenmeister, M.; Wang, J.; Wade, K. *Stud. Surf. Sci. Catal*. **1991**, *69*, 485.
(8) Yun, S. K.; Pinnavaia, T. J. *Inorg. Chem*. **1996**, *35*, 6853.
(9) Cheng, S.; Lin, J. T. In *Synthesis of Microporous Materials, Vol. II. Expanded Clays and Other Microporous Solids*; Occelli, M. L., Robson, H. E., Eds.; Van Nostrand Reinhold: New York, 1992; p 170.
(10) Drezdzon, M. A. *Inorg. Chem*. **1988**, *27*, 4628.
(11) Rives, V.; Ulibarri, M. A. *Coord. Chem. Rev*. **1999**, *181*, 61.
(12) Rives, V. In *Layered Double Hydroxides: Present and Future*; Rives, V., Ed.; Nova Science Publishers, Inc.: New York, 2001.

10.1021/ic034034u CCC: $25.00
Published on Web 06/04/2003

process. Metal oxalates are used as precursors for the preparation of metal oxide nanoparticles, using controlled thermal decomposition. Such complexation prevents, at medium-range temperatures, the crystallization of oxide particles.[13]

Besse et al.[14,15] have prepared solids of this family containing $[M^{III}(C_2O_4)_3]^{3-}$ and $[M^{II}(C_2O_4)_2]^{2-}$ in the interlayer space of Zn,Al−Cl LDHs by ion exchange, concluding that the experimental conditions during synthesis control the type of interlayer anion in the final solids. Polyphasic solids are obtained for systems containing Cu^{2+} and Zn^{2+}, due to the ease with which these cations form the corresponding oxalates, $M(C_2O_4)$. Gutmann et al.[16] have prepared Zn,Cr hydrotalcites with similar anionic complexes, such as $Cr[(mal)_3]^{3-}$ and *cis*-$Cr[(mal)_2(H_2O)_2]^{3-}$, and have followed the exchange by FT-IR spectroscopy. Carlino et al.[17] have intercalated $[Fe(C_2O_4)_3]^{3-}$ in a Mg,Al hydrotalcite, although in this case total carbonate/complex exchange was not reached.

In this work, we report on the incorporation of $[Cr(C_2O_4)_3]^{3-}$ in the interlayer space of a Mg,Al hydrotalcite following the anion exchange and reconstruction methods, using the nitrate and carbonate forms as the respective precursors. The solids have been characterized using different physicochemical techniques, and their thermal stability has been also studied.

Experimental Section

Synthesis of the Samples. The precursor LDHs have been prepared with a molar Mg/Al ratio of 2. The sample with interlayer carbonate, named MgAlC, was obtained following the method described by Reichle,[18] while the nitrate sample, MgAlN, was prepared using decarbonated water and a NaOH aqueous solution to maintain an adequate pH value.[19] The $K_3[Cr(C_2O_4)_3]\cdot 3H_2O$ complex was prepared from $K_2C_2O_4\cdot H_2O$, $H_2C_2O_4\cdot 2H_2O$, and $K_2Cr_2O_7$, following the method described in the literature.[20]

Incorporation of $[Cr(C_2O_4)_3]^{3-}$ in the interlayer space was carried out by anion exchange from the nitrate precursor, MgAlN, and by reconstruction of the solid obtained upon calcination of precursor MgAlC at 500 °C in nitrogen.

The sample prepared by reconstruction was obtained by calcining 2 g of the MgAlC precursor at 500 °C for 3 h in nitrogen. The solid formed was added to an aqueous solution formed by 3.07 g of $K_3[Cr(C_2O_4)_3]\cdot 3H_2O$ dissolved in 100 mL of decarbonated water. The magnetically stirred suspension was heated at 50 °C for 6 h in a nitrogen atmosphere. The filtered solid was washed several times with decarbonated water by centrifugation and was dried in an oven at 50 °C. The green solid will be labeled as MgAlCrR. Before filtration, a portion of the suspension was submitted to hydrothermal treatment in a Teflon lined stainless steel bomb at autogenous pressure at 70 °C for 15 days, and then it was washed by centrifugation and filtered as described, leading to sample MgAlCrRH.

To prepare the sample by anion exchange, a solution formed by 8.6 g of $K_3[Cr(C_2O_4)_3]\cdot 3H_2O$ dissolved in 100 mL of decarbonated water was added to 100 mL of the MgAlN suspension (containing ca. 5 g of solid). The mixture was heated at 50 °C for 9 h in a nitrogen atmosphere, while it was magnetically stirred. The precipitate formed was washed with decarbonated water by centrifugation, filtered, and dried at room temperature, leading to sample labeled as MgAlCrI. All samples containing chromium show a characteristic green color.

Characterization Techniques. Elemental chemical analyses for Mg, Al, and Cr were carried out in Servicio General de Análisis Químico (University of Salamanca, Spain) by atomic absorption in a Mark 2 ELL-240 instrument after dissolving the samples in nitric acid. Carbon analysis was carried out in a Leco, model CHNS 832, elemental analyzer.

Powder X-ray diffraction diagrams (PXRD) were collected on a Siemens D-500 using Cu Kα radiation ($\lambda = 1.54050$ Å) and quartz as an external standard.

Fourier transform Infrared spectra (FT-IR) were collected in a Perkin-Elmer FT-1730 instrument using the KBr pellet technique; 100 scans were averaged to improve the signal-to-noise ratio, at a nominal resolution of 4 cm^{-1}.

Differential thermal analyses (DTAs) and thermogravimetric analyses (TGs) were measured on DTA7 and TG7 instruments, respectively, from Perkin-Elmer. The analyses were carried out in flowing (30 mL/min) oxygen from L'Air Liquide (Spain).

The UV−vis spectra of the samples were recorded following the diffuse reflectance technique (UV−vis/DR) in a Shimadzu UV-240 spectrophotometer, using 5 nm slits and MgO as a reference.

Temperature-programmed reduction (TPR) analysis was carried out on the samples, without any pretreatment, in a Micromeritics TPR/TPD 2900 instrument, at a heating rate of 10 °C/min, using ca. 15 mg of sample and 60 mL/min of a H_2/Ar mixture (5 vol %, from L'Air Liquide, Spain) as reducing agent. Experimental conditions for TPR runs were chosen according to data reported elsewhere[21] in order to reach a good resolution of the component peaks.

Specific surface areas were measured following the single-point method, in a Micromeritics Flow-sorb II-2300 apparatus. The nitrogen adsorption−desorption isotherms were recorded at −196 °C in a Gemini instrument, from Micromeritics, on samples previously degassed at 150 °C for 2 h by passing a nitrogen flow (from L'Air Liquide, Spain) in a Flow Prep 060 apparatus, also from Micromeritics.

Surface acidity monitoring was carried out through FT-IR spectroscopy study of pyridine adsorption in a Perkin-Elmer 16PC spectrometer coupled to a high-vacuum Pyrex system, and using self-supported disks, degassed in situ in a special cell (built in Pyrex, but with CaF_2 windows, transparent to the IR radiation in the required wavenumbers range) at 400 °C for 2 h, previous to pyridine adsorption. The spectrometer is coupled to a PC, and commercial software was used to process the spectra. There were 100 scans taken to improve the signal-to-noise ratio, at a nominal resolution of 2 cm^{-1}. The gas is admitted to the IR-adsorption cell at room temperature, and after 15 min for equilibration, the gas phase is removed by outgassing at different temperature (100−400 °C) and the spectrum is recorded.

(13) Traversa, E.; Nunziante, P.; Chiozzini, G. *Thermochim. Acta* **1992**, *199*, 25.
(14) Prevot, V.; Forano, C.; Besse, J. P. *J. Mater. Chem.* **1999**, *9*, 155.
(15) Prevot, V.; Forano, C.; Besse, J. P. *J. Solid. State Chem.* **2000**, *153*, 301.
(16) Gutmann, N.; Müller, B.; Tiller, H. J. *J. Solid State Chem.* **1995**, *119*, 331.
(17) Carlino, S.; Hudson, M. J. *Solid State Ionics* **1998**, *110*, 153.
(18) Reichle, W. T. *J. Catal.* **1980**, *63*, 295.
(19) Del Arco, M.; Gutiérrez, S.; Martín, C.; Rives, V.; Rocha, J. *J. Solid State Chem.* **2000**, *151*, 272.
(20) Bailar, J. C., Jr.; Jones, E. M. *Inorg. Synth.* **1939**, *1*, 37.
(21) Malet, P.; Caballero, A. *J. Chem. Soc., Faraday Trans 1* **1988**, *84*, 2369.

Table 1. Elemental Chemical Analysis Data

sample	Mg/Al[a]	Al/Cr[a]	$C_2O_4^{2-}$/Cr[a]
MgAlC	1.94		
MgAlN	1.98		
$K_3[Cr(C_2O_4)_3]\cdot 3H_2O$			2.99
MgAlCrR	1.86	2.40	2.01
MgAlCrRH	1.46	1.98	1.43
MgAlCrI	1.98	3.03	2.95

[a] Molar ratio.

Results and Discussion

Chemical Composition. Elemental chemical analysis results led to the molar ratios for some relevant pairs of the components of the solids prepared and included in Table 1. The molar Mg/Al ratio in the starting precursors is maintained in sample MgAlCrI (1.98, the same value as in sample MgAlN), but it decreases to 1.86 (from the initial value 1.94 for sample MgAlC) for the chromium-containing sample prepared by reconstruction, MgAlCrR, and further to 1.46 for the hydrothermally treated sample, MgAlCrRH. These results suggest that a portion of magnesium is lost during the synthesis of the compounds. With respect to the oxalate/Cr molar ratio, the value measured for sample MgAlCrI is acceptably similar to that in the complex. However, drastic decreases are observed for samples MgAlCrR and MgAlCrRH. With respect to the aluminum content, measured through the Al/Cr molar ratio, the expected value is three, as each three-valent interlayer anion should balance three aluminum cations from the layers. The value measured for sample MgAlCrI is very close to this value (3.03, only 1% deviation), but again, the value decreases for the other two samples, MgAlCrR (2.40) and MgAlCrRH (1.98), indicating these two routes (reconstruction, and reconstruction plus hydrothermal treatment) are not adequate ones to prepare $[Cr(C_2O_4)_3]^{3-}$-intercalated Mg,Al hydrotalcite. Probably, the reaction conditions lead to a partial decomposition of the complex.

So, $NO_3^-/[Cr(C_2O_4)_3]^{3-}$ exchange is complete for sample MgAlCrI, for which the formula $[Mg_{0.664}Al_{0.336}(OH)_2][Cr(C_2O_4)_3]_{0.112}\cdot 0.67H_2O$ can be given (the water content has been determined from the TG measurements). The empirical formulas have not been determined for samples MgAlCrR and MgAlCrRH, as different phases exist in these two solids.

Powder X-ray Diffraction. The PXRD diagrams for samples MgAlCrR and MgAlCrI, together with those of the corresponding precursors (MgAlC and MgAlN), are shown in Figure 1. The positions recorded for the diffraction maxima coincide with those expected for a hydrotalcite, assuming a 3R symmetry.[22−24] From these values, cell parameters were calculated, obtaining the values $a = 3.05$ Å and $c = 29.7$ Å for sample MgAlCrI, and 3.03 and 30.24 Å for sample MgAlCrR. The value of a has been calculated from the position of the (110) peak (the first of the couple close to $2\theta = 60°$), while the value of c has been averaged from the positions of the three harmonics due to basal planes (003), (006), and (009) at lower diffraction angles.

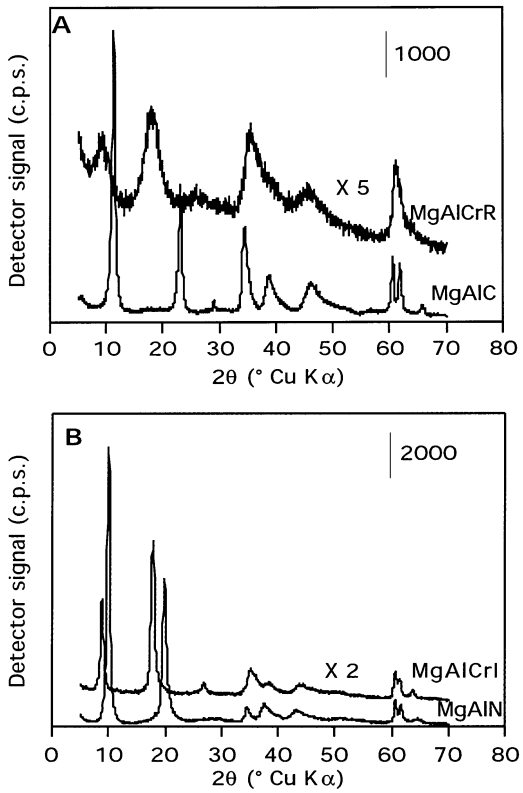

Figure 1. Powder X-ray diffraction diagrams of (A) sample MgAlCrR and precursor MgAlC, and (B) sample MgAlCrI and sample MgAlN.

The d-spacings corresponding to planes (003) were 9.9 and 10.08 Å, respectively, for samples MgAlCrI and MgAlCrR. These values are very close to those previously reported by Besse et al.[15] for hydrotalcites containing tris-oxalate complexes in the interlayer space. Carlino et al.[17] have reported values slightly larger for a Mg,Al hydrotalcite intercalated with $[Fe(C_2O_4)_3]^{3-}$ species, due to the simultaneous presence of carbonate in the interlayer space, together with the complex anion. The PXRD diagram for sample MgAlCrRH (not shown) is similar to that from sample MgAlCrR, although the diffraction maxima are stronger.

If the width of the brucite-like layer (4.8 Å)[10] is subtracted from the d-spacing recorded for these samples (9.99 ± 0.09 Å), the value obtained is coincident, within experimental error, with the height of the $[Cr(C_2O_4)_3]^{3-}$ anion (calculated by application of program CS Chem 3D Pro); that is, the anion should be oriented with one of its C_2 axes perpendicular to the brucite-like layers, Figure 2. Probably, this orientation permits a maximum interaction with the layers through hydrogen bonding with the layer hydroxyl groups.

Incorporation of bulk anions in the interlayer space of hydrotalcites sometimes gives rise to an increased turbostratic disorder, thus leading to asymmetric diffraction maxima above ca. $2\theta \geq 25°$. In our case, incorporation of $[Cr(C_2O_4)_3]^{3-}$ does not give rise to important changes in the shape of the maxima recorded, suggesting a rather good ordering of the layers along the c-axis. These results are similar to those previously reported by Gutmann et al.[16] upon intercalation of $[Cr(mal)_3]^{3-}$ in the interlayer of a Zn,Cr hydrotalcite.

(22) Bookin, A. S.; Cherkashin, V. I.; Drits, V. *Clays Clay Miner*. **1993**, *41*, 558.
(23) Bookin, A. S.; Drits, V. *Clays Clay Miner*. **1993**, *41*, 551.
(24) Gay, P. *The Crystalline State. An Introduction*, 3rd ed.; Oliver and Boyd: Edinburgh, 1972.

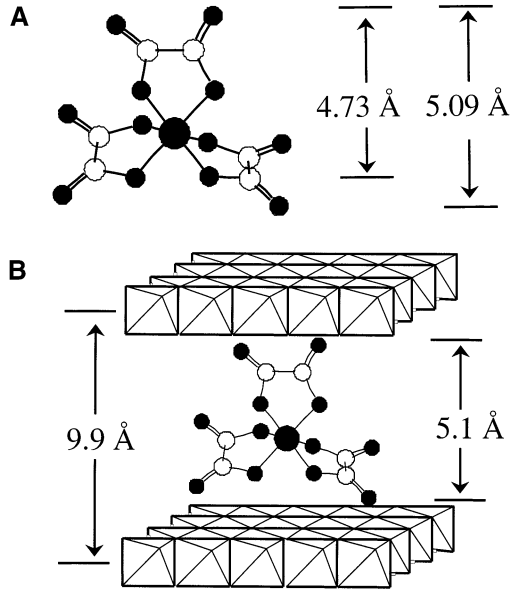

Figure 2. Molecular dimensions of free $[Cr(C_2O_4)_3]^{3-}$ anion and that intercalated between the sheets of the layered double hydroxide.

On comparing the PXRD diagrams shown in Figure 1, an inversion in the relative intensities of the maxima due to diffraction by planes (003) and (006) is observed when passing from the hydrotalcite precursor (MgAlN and MgAlC) to the corresponding solids with intercalated $[Cr(C_2O_4)_3]^{3-}$. Such behavior has been previously reported by other authors for hydrotalcites containing chromate, vanadate, or silicate in the interlayers[19,25−27] and has been related to an increase in the electron density in the (00*l*) planes at a distance equal to one-half of the spacing of the (003) planes.[14]

FT-IR Spectroscopy. FT-IR spectroscopy is very helpful for the study of hydrotalcites, especially those containing interlayer organic anions (or anions with organic moieties), as it is very sensitive to the symmetry of the organic anion and to the interactions of the anion with its environment; in the case of oxalate complexes, also hydrogen bonding and coordination bonding can be studied by application of this technique.[28−30] Local symmetry of oxalate in potassium oxalate is D_{2h} and shows two IR-active ν(CO) modes, the corresponding bands observed at 1594 and 1310 cm^{-1} being due to the ν_{as}(COO) and ν_s(COO) stretching modes of the carboxylate groups. The bands are recorded at 1630, 1380, and 1330 cm^{-1} for magnesium oxalate. However, when bonded to a metal cation forming a coordination compound, and acting as a bidentate ligand, the local symmetry decreases to C_{2v}, and then, four bands should be expected in the IR spectrum due to the C−O stretching modes.

The FT-IR spectra of the free complex (as a potassium salt) and of the three hydrotalcites with the intercalated complex are shown in Figure 3. Only the 1800−300 cm^{-1} range is shown, as this is the range where the most characteristic bands of the complex are recorded. Ascription of the most representative bands is summarized in Table 2.[30]

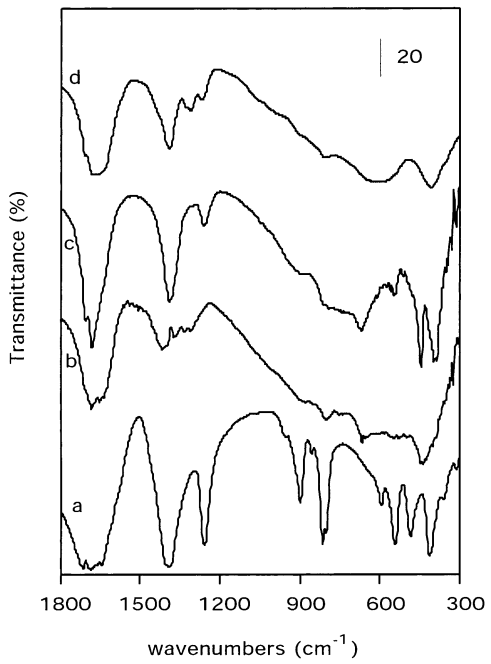

Figure 3. FT-IR spectra of (a) $K_3[Cr(C_2O_4)_3]\cdot 3H_2O$; (b) sample MgAlCrRH; (c) sample MgAlCrI; and (d) sample MgAlCrR.

Table 2. Infrared Spectroscopic Data (cm^{-1}) and Assignments for $K_3[Cr(C_2O_4)_3]\cdot 3H_2O$ and the $[Cr(C_2O_4)_3]^{3-}$-Intercalated Hydrotalcite

assignment	$K_3[Cr(C_2O_4)_3]\cdot 3H_2O$	MgAlCrI	MgAlCrR
ν_{as}(C═O)	1710, 1686, 1660	1705, 1688, 1660(sh)[a]	1709, 1663, 1640[b]
ν_s(CO) + ν_s(C−C)	1391	1385	1390, 1330[b]
ν_s(CO) + δ(O−C═O)	1258, 898	1261, 897	1265, 893
δ(O−C═O) + ν(Cr−O)	812	812(sh)	805
ν(Cr−O) + ν_a(C−C)	543	543(sh)	540(sh)
ν(Mg−O, Al−O...)		670, 446, 398	660, 448, 398
ν(Cr−O)	415		

[a] sh = shoulder. [b] ν_{as}(COO) and ν_s(COO) of $Mg(C_2O_4)$.

Most of the characteristic bands of the complex are also recorded in the FT-IR spectrum of sample MgAlCrI (see Table 2). Some of them, especially those due to the antisymmetric CO modes of oxalate, are shifted with respect to their positions in the spectrum of the potassium complex, probably because of the restrictions within the interlayer space and the rather strong interaction with the hydroxyl groups via hydrogen bonding.[14]

The bands recorded at 1385 and 1261 cm^{-1} are ascribed to the ν_s(CO) stretching modes of oxalate and, although weaker, are recorded in positions very close to those of the free complex. The shoulder at 812 cm^{-1} is due to the combination ν(Cr−O) + δ(O−C═O). The broad bands recorded below 800 cm^{-1} are due to Mg−O and Al−O vibration modes of the brucite-like layers,[31] which do not permit a clear identificaction of the band due to the Cr−O stretching mode, recorded at 415 cm^{-1} for the free complex.

(25) Kwon, T.; Pinnavaia, T. J. *Chem. Mater*. **1989**, *1*, 381.
(26) Kooli, F.; Rives, V.; Ulibarri, M. A. *Inorg. Chem*. **1995**, *34*, 5114.
(27) Kooli, F.; Rives, V.; Ulibarri, M. A. *Inorg. Chem.* **1995**, *34*, 5122.
(28) Schmelz, J.; Miyazawa, T.; Mizushima, S. I.; Lane, T. J.; Quagliano, J. V. *Spectrochim. Acta* **1957**, *9*, 51.
(29) Fujita, J.; Martell, A. L.; Nakamoto, K. *J. Chem. Phys*. **1962**, *36*, 324.
(30) Nakamoto, K. *Infrared and Raman Spectra of Inorganic and Coordination Compounds*, 5th ed.; Wiley: New York: 1997.

A detailed analysis of the FT-IR spectrum of sample MgAlCrR suggests the presence of additional phases, in addition to the expected $[Cr(C_2O_4)_3]^{3-}$-containing Mg,Al hydrotalcite. It should be stressed that the presence of this layered material is definitively concluded from the PXRD diagram shown in Figure 1, but the results of the elemental chemical analysis suggest that it is not the only solid in the sample; probably, other components are mostly amorphous or exist in a rather low concentration and so are undetectable by PXRD. For MgAlCrR, bands at 1700−1660 cm^{-1} are due to the antisymmetric ν_{as}(C═O) vibration of bidentate oxalate, while those due to the ν_s(CO) mode of the chromium complex are recorded at 1390 and 1265 cm^{-1}. In addition, two other bands are recorded at 1640 and 1330 cm^{-1}, which were absent in the spectra of $K_3[Cr(C_2O_4)_3]\cdot 3H_2O$ and of sample MgAlCrI. The positions of these bands coincide with those due to modes ν_{as}(COO) and ν_s(COO) of magnesium oxalate. So, the presence of this compound in sample MgAlCrR can be tentatively concluded. Its formation can be due to partial hydrolysis of the chromium complex at the high pH (larger than 8) given to the solution by the MgAlC precursor calcined at 500 °C during the reconstruction process. This process would also account for the rather low oxalate/Cr ratio in this sample: if the complex is partially decomposed, some of the oxalate anions (in addition to those reacting with Mg^{2+} cations producing insoluble magnesium oxalate) would be in solution and removed during washing, while chromium would precipitate as amorphous oxohydroxides, undetectable by PXRD. Nevertheless, the content of magnesium oxalate in the final solid should be rather low, as it is not detected at all by PXRD.

The band at 1260 cm^{-1} due to the ν_s(COO) mode of bidentate oxalate is no longer recorded in the FT-IR spectrum of sample MgAlCrRH, suggesting this synthesis procedure leads to destruction of the complex. This result is opposite to the results obtained by PXRD for this sample, which indicated that the layered structure, with a basal spacing close to 10 Å, actually exists in the sample. We can tentatively assume that it corresponds to a MgAl hydrotalcite with intercalated oxalate units formed upon decomposition of the complex, as the spacing is very close to those previously reported[14,32] for Zn−Cr, Zn−Al, and Mg−Al with upward-oriented, oxalate intercalates.

Thermal Decomposition. The study of the thermal decomposition has been carried out only on sample MgAlCrI, for which the FT-IR spectrum, PXRD diagram, and results from elemental chemical analysis strongly suggest that it is constituted by a well-defined hydrotalcite. We have studied the DTA and TG diagrams for this sample, recorded in oxygen. In addition, and in order to identify the stable phases formed along thermal decomposition, we have also recorded the PXRD diagrams and the FT-IR spectra of solids calcined at given temperatures for 2 h; these solids will be hereafter named as MgAlCrI/*T*, where *T* stands for the calcination temperature, in degrees Celsius. Also, in order to permit an easier interpretation of the thermal decomposition curves, these have been recorded also for $K_3[Cr(C_2O_4)_3]\cdot 3H_2O$. Both sets of curves are shown in Figure 4.

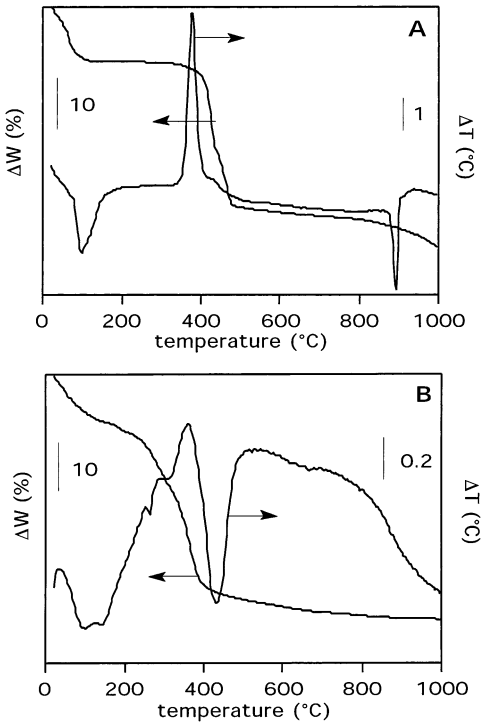

Figure 4. Differential thermal analysis and thermogravimetric analysis curves of (A) $K_3[Cr(C_2O_4)_3]\cdot 3H_2O$ and (B) sample MgAlCrI.

The DTA curve of the chromium complex, Figure 4A, exhibits three thermal effects although only two weight losses are recorded in the TG curve. The magnitude of the weight loss was not valuable to determining the processes taking place during decomposition as, unfortunately, we could not analyze the gases evolved during thermal decomposition. The first weight loss, with a corresponding endothermic peak at 105 °C, is due to removal of crystallization water; the main weight loss is composed of two consecutive processes, giving rise to an exothermic peak at 381 °C, immediately followed by a weaker shoulder at 441 °C. The phases identified by PXRD after these processes were K_2CrO_4 and $K_2C_2O_4$; this last decomposes to K_2CO_3, whose melting is responsible for the sharp endothermic peak (without weight loss) at 894 °C. These compounds have been identified by PXRD and FT-IR spectroscopy in the solids calcined at temperatures immediately above the DTA effects.

The FT-IR spectrum of the calcined chromium complex does not change when calcination is performed below 340 °C. Above this temperature, together with the bands already described, new bands are recorded at 1600, 1310, and 889 cm^{-1}, Figure 5. The first two bands correspond to ν_{as}(COO) and ν_s(COO) modes of monodentate oxalate, as in $K_2C_2O_4$, and the third band to ν(Cr−O) of K_2CrO_4;[33] it should be noted that the solid calcined at this temperature is light yellow, and not green. Upon calcination at 450 °C, the bands due to ν_{as}(COO) of bidentate oxalate (1713−1660 cm^{-1})

(31) Kloprogge, J. T.; Frost, R. L. In *Layered Double Hydroxides: Present and Future*; Rives V., Ed.; Nova Science Publishers, Inc.: New York, 2001; Chapter 5, p 139.
(32) Meyn, M.; Beneke, K.; Lagaly, G. *Inorg. Chem.* **1990**, *29*, 5201.
(33) Weinstock, N.; Schulze, H.; Müller, A. *J. Chem. Phys.* **1973**, *59*, 5063.

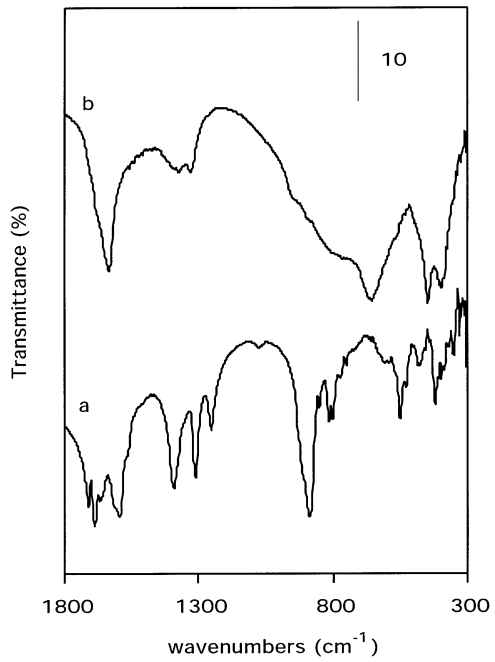

Figure 5. FT-IR spectra of (a) $K_3[Cr(C_2O_4)_3]\cdot 3H_2O$ calcined at 340 °C, and (b) sample MgAlCrI calcined at 300 °C.

disappear; in addition to the bands due to potassium oxalate, other new bands are recorded at 1478, 1450, 1379, and 1061 cm^{-1}. The band at 1379 cm^{-1} is characteristic of carbonate, thus suggesting total decomposition of oxalate at this temperature.

The DTA diagram for sample MgAlCrI, Figure 4B, shows a broad, complex, endothermic effect, with two minima at 100 and 144 °C. This peak is usually ascribed[34] to removal of interlayer water molecules from the hydrotalcite structure, and the corresponding weight loss (9.84%) has been used to determine the water content in this sample. Above this temperature, an exothermic effect (similar to that recorded for $K_3[Cr(C_2O_4)_3]$) is recorded, but it immediately overlaps with a strong endothermic effect, due to total decomposition of the complex, and dehydroxylation of the brucite-like layers is recorded.

The PXRD diagrams of sample MgAlCrI calcined in air at different temperatures are shown in Figure 6. Calcination up to 200 °C does not significantly change the shape and appearance of the diagram; only a slight decrease in the interlayer space has been observed. Such a process has been observed previously, and it has been ascribed[34] to removal of interlayer water molecules, which might take place with simultaneous anchoring (grafting) of interlayer oxygen-containing anions to the brucite-like layer. The peaks become broader, and the layered structure seems to be detected even after calcining at 300 °C. Above this temperature, the structure seems to be absolutely destroyed, and only very broad and weak maxima, typical of amorphous species, are recorded in the PXRD diagram. When the calcination temperature is further increased, broad peaks close to the

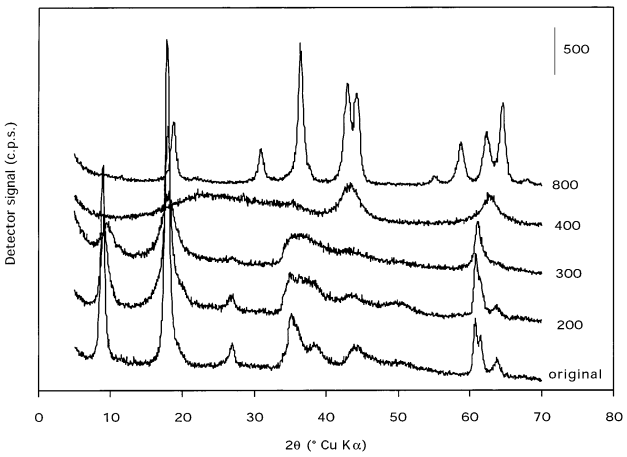

Figure 6. PXRD diagrams of original sample MgAlCrI and sample calcined in air at the temperatures given (in °C).

positions expected for periclase (MgO) are recorded; their sharpness and intensity increase with the calcination temperature, and from 700 °C, new peaks due to $MgAl_{1.5}Cr_{0.5}O_4$, with the spinel structure, whose intensity further increases with the calcination temperature, are recorded in addition to the MgO peaks. A parallel study by FT-IR spectroscopy of the calcined samples indicates that the complex is stable in the interlayer up to 200 °C, as the spectrum for sample MgAlCrI/200 is very similar to that of parent MgAlCrI. As shown in Figure 5, above this temperature the characteristic bands of bidentate oxalate at 1705−1640 cm^{-1} merge in a single band at 1635 cm^{-1}, which is recorded together with other bands at 1406, 1376, and 1330 cm^{-1}. Some of these bands are similar to those recorded for samples MgAlCrR and MgAlCrRH, and to those of the free complex calcined at 450 °C, suggesting that, also in this case, calcination has given rise to transformation from bidentate to monodentate oxalate and to carbonate. Although the Cr−O stretching band at 899 cm^{-1} is not recorded, formation of chromate-like species should be also concluded for this sample, because of its light yellow color.

UV−Vis Spectroscopy. The UV−vis spectrum of sample MgAlCrI, recorded by the diffuse reflectance technique, is shown in Figure 7. The spectrum of the free complex (as a potassium salt, not shown in the figure) shows bands which can be easily ascribed to spin-allowed, Laporte-forbidden transitions from the fundamental state $^4A_{2g}(F)$ to $^4T_{2g}(F)$ and $^4T_{1g}(F)$, together with a third transition to $^4T_{1g}(P)$.[35] In addition, a very weak band is also recorded at 695 nm, which can be ascribed to a spin-forbidden transition, known as "ruby line" because of its extreme narrowness which was first observed for this mineral.[36]

The bands observed in the UV−vis spectrum of sample MgAlCrI are very similar to those for the free complex,[35] except that the third band (due to transition $^4A_{2g}(F) \rightarrow {}^4T_{1g}(P)$) is recorded as a shoulder of the strongest band due to a $O^{2-} \rightarrow M^{n+}$ charge-transfer process. From the positions

(34) Rives, V. In *Layered Double Hydroxides: Present and Future*; Rives V., Ed.; Nova Science Publishers, Inc.: New York, 2001; Chapter 4, p 115.

(35) Lever, A. B. P. *Inorganic Electronic Spectroscopy*, 2nd ed.; Elsevier: Amsterdam, 1984.

(36) Eaton, S. S.; Yager, T. D.; Eaton, G. R. *J. Chem. Educ.* **1979**, *56*, 635.

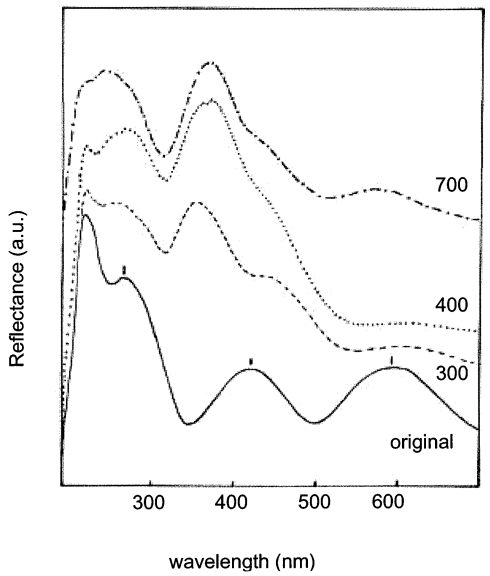

Figure 7. UV−vis/DR spectra of original sample MgAlCrI and sample calcined in air at the temperatures given (in °C).

of the first and second maxima, close to 580 and 420 nm, respectively, and using the formula by Dou,[37] the spectral parameters for the intercalated complex have been calculated, $\Delta_0 = 17500\ cm^{-1}$, and B (Racah parameter) $= 598\ cm^{-1}$; the expected position for the third band has been calculated, obtaining a value, 252 nm, very close to that recorded for the free complex. Similar spectra are recorded for the sample calcined up to 200 °C.

However, when the sample is calcined at 250 °C, a shift of the band originally recorded at 420 nm toward lower wavelength is observed, now being recorded at 370 nm. The shape of the spectrum is deeply modified upon calcination at 300 °C: the band around 600 nm has almost completely disappeared, and the spectrum is dominated by a strong absorption at 352 nm (in addition to the band at 252 nm), together with a shoulder at ca. 424 nm. The intensity of this shoulder decreases when the calcination temperature is increased to 400 °C; at this temperature, the spectrum shows two bands at 268 and 368 nm, analogous to those recorded for K_2CrO_4, for which the bands are recorded at 272 and 369 nm.[38] These results further confirm that an oxidation from Cr^{3+} to Cr^{6+} takes place during calcination, as previously suggested by the TG/DTA and FTIR data. A further increase in the calcination temperature to 700 °C gives rise to development of the band at 580 nm, characteristic of Cr^{3+} species in an octahedral coordination, thus suggesting reduction from Cr^{6+} to Cr^{3+}. However, although a shoulder close to 420 nm again develops, the strong band at ca. 350 nm is still recorded. Probably, formation of the $MgAl_{1.5}Cr_{0.5}O_4$ spinel gives rise to Cr^{3+} cations in tetrahedral and octahedral sites, thus accounting for this rather complex spectrum, although the contribution of Cr^{6+} species, still existing in this sample calcined at 700 °C (see TPR results) cannot be ignored.

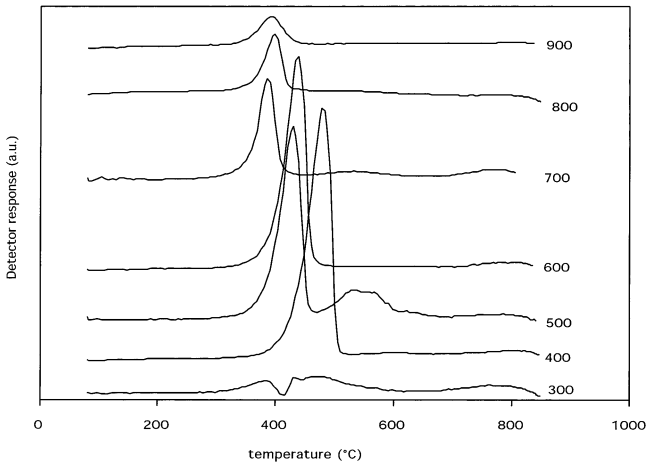

Figure 8. TPR diagrams of sample MgAlCrI calcined in air at the temperatures given (in °C).

Temperature-Programmed Reduction. According to the data reported in preceding paragraphs, decomposition of the interlayer chromium complex in air takes place with the simultaneous oxidation of Cr^{3+} species to Cr^{6+}, which are reduced again to Cr^{3+} when the calcination temperature is further increased. In order to analyze these changes, the reduction profiles of original and calcined MgAlCrI/*T* samples have been studied by TPR; representative curves are included in Figure 8. Previous results[39] have shown that, during TPR analysis in the same conditions used here, MgAl-carbonate and MgCr-carbonate hydrotalcites do not undergo any reduction; consequently, hydrogen consumption in our samples should be exclusively due to reduction if chromium ions are in an oxidation state higher than +3.

The TPR curves for the original MgAlCrI sample and for the samples calcined up to 200 °C do not show any reduction band below 850 °C, in agreement with previous results for other chromium-containing hydrotalcites.[39−42]

However, when the precalcination temperature is raised, reduction processes take place. So, an intense reduction band is recorded at ca. 460 °C, whose intensity reaches a maximum for the sample precalcined at 400 °C. A further increase in the precalcination temperature leads to a slight shift of the reduction band to lower temperatures, and to a decrease in its intensity, finally almost disappearing when the sample is precalcined at 900 °C. According to the results obtained by application of the other experimental techniques used, this band should be ascribed to reduction of chromate-like species formed during calcination at intermediate calcination temperatures, as also confirmed by development of the UV−vis band close to 600 nm in the spectra of the sample calcined at this high temperature.

Hydrogen consumption along the TPR runs has been calculated from the area under the reduction curve. The results have been included in Table 3, where the positions

(37) Dou, Y. *J. Chem. Educ*. **1990**, *67*, 134.
(38) Fuda, K.; Suda, K.; Matsunaga, T. *Chem. Lett*. **1993**, 1479.
(39) Rives, V.; Ulibarri, M. A.; Montero, A. *Appl. Clay Sci*. **1995**, *10*, 83.
(40) Del Arco, M.; Galiano, M. V. G.; Rives, V.; Trujillano, R.; Malet, P. *Inorg. Chem*. **1996**, *35* 6362.
(41) Del Arco, M.; Rives, V.; Trujillano, R.; Malet, P. *J. Mater. Chem*. **1996**, *6*, 1419.
(42) Labajos, F. M.; Rives, V. *Inorg. Chem*. **1996**, *35*, 5313.

Table 3. Summary of TPR Data: Position of the Reduction Maximum, Molar H_2/Cr Ratio, and Percentage of Reduced Cr(VI)

sample	*T*/°C	H_2/Cr[a]	% Cr^{VI}
MgAlCrI/300	465	0.01	2.2
MgAlCrI/400	457	1.50	100.0
MgAlCrI/500	434	1.43	95.3
MgAlCrI/600	434	1.15	77.1
MgAlCrI/700	409	0.58	38.6
MgAlCrI/800	395	0.28	18.6
MgAlCrI/900	395	0.21	14.1

[a] Molar ratio.

Table 4. Specific Surface Area ($m^2\ g^{-1}$) and Crystallographic Phases of the Calcined MgAlCrI Samples

sample	S_{BET}	crystallographic phase
MgAlN	3	HT
MgAlCrI	53	HT
MgAlCrI/100	52	HT
MgAlCrI/200	52	HT
MgAlCrI/300	61	HT[a]
MgAlCrI/400	82	MgO[a]
MgAlCrI/500	76	MgO
MgAlCrI/600	76	MgO
MgAlCrI/700	77	MgO + $MgAl_{1.5}Cr_{0.5}O_4$[a]
MgAlCrI/800	62	MgO + $MgAl_{1.5}Cr_{0.5}O_4$[a]
MgAlCrI/900	53	MgO + $MgAl_{1.5}Cr_{0.5}O_4$

[a] Poorly crystallized.

of the maxima are given together with the molar H_2/Cr ratio; from these values, the percentage of Cr^{6+} reduced has been calculated, according to the following reaction:

$$2Cr^{6+} + 3H_2 \rightarrow 2Cr^{3+} + 6H^+$$

As these results show, all chromium has been oxidized to the Cr^{6+} state upon calcination at 400 °C, sample MgAlCrI/400, as the molar H_2/Cr ratio equals 1.5, the theoretical value expected from the reaction shown. This oxidation percentage steadily decreases as the calcination temperature is increased, as a consequence of the reduction from Cr^{6+} to Cr^{3+} even under an oxidant atmosphere. It should be pointed out that even at 700 °C ca. 40% of chromium seems to exist in the +6 state, thus probably accounting for the absorption band in the UV−vis spectrum at ca. 350 nm. Fuda et al.[38] have studied the $Cr^{3+} \rightarrow Cr^{6+}$ oxidation during thermal decomposition of hydrotalcites containing Cr^{3+} species in the layers, concluding that the presence of interlayer carbonate favors such an oxidation; some of us have previously reported[40,41] that such an oxidation is, however, hindered if anions other than carbonate (e.g., oxovanadate) exist in the interlayer space.

Surface Texture Studies. Specific surface areas of the original and calcined samples, as determined following the BET method, are included in Table 4. The crystallographic phases determined by PXRD for these samples are also listed in this table. The value determined for the uncalcined sample ($53\ m^2\ g^{-1}$) does not change as the calcination temperature is increased up to 200 °C. The isotherms correspond to type II in the IUPAC classification, characteristic of macroporous adsorbents, with unrestricted monolayer−multilayer adsorption,[43] thus indicating that the nitrogen molecules are not able to enter the interlayer space, probably because this is very much "populated" by the $[Cr(C_2O_4)_3]^{3-}$ anions. For all samples, the external surface areas[44] coincide with the values calculated by application of the t-method by de Boer,[45] confirming the absence of detectable micropores.

The specific surface area increases when the calcination temperature increases above 200 °C, where, according to the PXRD diagrams in Figure 6, destruction of the layered structure and formation of mostly amorphous solids starts. A maximum S_{BET}, $82\ m^2\ g^{-1}$, is obtained for the sample calcined at 400 °C, where only rather poorly crystallized MgO is detected by PXRD, together with amorphous chromate, oxalate, and carbonate, detected by other experimental techniques. When crystallization is improved, first forming only MgO, and forming also $MgAl_{1.5}Cr_{0.5}O_4$ at higher temperatures, the specific surface area steadily decreases, reaching, at 900 °C, a value rather close to that of the starting material.

Changes in the specific surface area are then undoubtedly related to changes in the crystallographic phases existing in the calcined solids. In addition, development of large specific surface areas at intermediate calcination temperatures has been related to formation of holes and chimneys in the layers when the interlayer anions decompose giving rise to volatile compounds (e.g., CO or CO_2 in our case).[46−48]

Surface Acidity. The solids obtained after calcination of hydrotalcites have shown their suitability as catalysts for different reactions.[1,49] Preliminary studies on the surface acidity of the solids studied here are reported. The study corresponds to a FT-IR monitoring of pyridine (py) adsorption on the samples calcined at temperatures above that required for destruction of the layered structure, as outgassing at 400 °C is required for a complete cleaning of the surface prior to py adsorption; otherwise the spectra are poorly resolved.

Adsorption of pyridine at room temperature and outgassing at the same temperature on sample MgAlCrI/500, Figure 9, gives rise to infrared absorption bands at 1604, 1588, 1575, 1489, and 1443 cm^{-1}, which can be ascribed to modes 8a, 8b, 19a, and 19b, respectively, of pyridine adsorbed on surface Lewis acid site.[50−53] Splitting of the band due to mode 8a (bands at 1604 and 1588 cm^{-1}) indicates the presence of two types of surface Lewis acid sites, probably surface coordinatively unsaturated Cr^{6+} and Mg^{2+} cations. Coordinatively unsaturated Mg^{2+} cations are weak acids, as after outgassing at 100 °C the band due to coordinated pyridine

(43) Sing, K. S. W.; Everett, D. H.; Haul, R. A. W.; Moscou, L.; Pierotti, R.; Rouquerol, J.; Sieminiewska, T. *Pure Appl. Chem*. **1985**, *57*, 603.
(44) Cranston, R. W.; Inkley, F. A. *Adv. Catal*. **1957**, *9*, 143.
(45) Lippens, B. C.; de Boer, J. H. *J. Catal*. **1965**, *4*, 319.
(46) Kruissink, E. C.; Van Reijden, L. L.; Ross, J. R. H. *J. Chem. Soc., Faraday Trans. 1* **1981**, *77*, 649.
(47) Reichle, W. T. *J. Catal.* **1985**, *94*, 547.
(48) Kagunya, W.; Jones, W. *Appl. Clay Sci*. **1995**, *10*, 95.
(49) Basile, F.; Vaccari, A. In *Layered Double Hydroxides: Present and Future*; Rives V., Ed.; Nova Science Publishers, Inc.: New York, 2001; Chapter 10, p 285.
(50) Cook, D. *Can. J. Chem.* **1961**, *39*, 2009.
(51) Parry, E. P. *J. Catal*. **1963**, *2*, 371.
(52) Bellamy, L. J. *The Infrared Spectra of Complex Molecules*; Chapman & Hall: London, 1975.
(53) Boehm, H. P.; Knozinger, H. In *Catalysis*; Anderson, J. R., Bonderot, M., Eds.; Springer: Berlin, 1983; Vol 4, p 40.

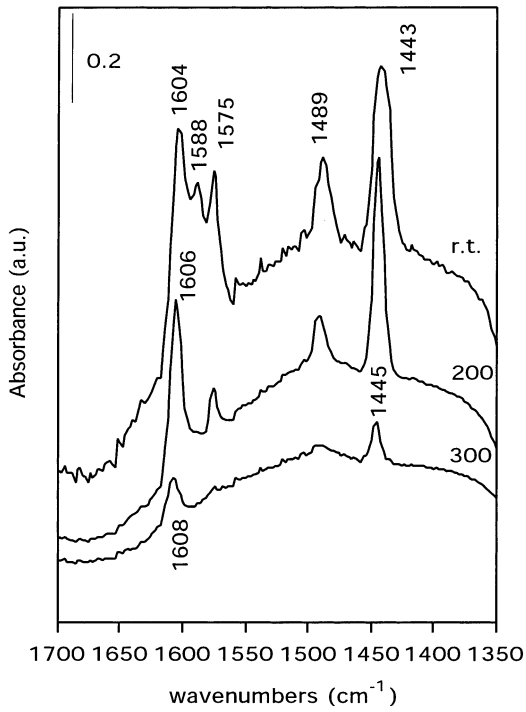

Figure 9. FT-IR spectra of pyridine adsorbed on sample MgAlCrI/500 at room temperature (rt) and outgassed at rt, 200 and 300 °C.

at 1588 cm^{-1} vanishes, while the other bands recorded slightly shift toward higher wavenumbers. The intensities of the bands also decrease, although very slightly below 300 °C, indicating the surface Lewis acid sites associated to Cr^{6+} ions are strong sites. However, no absorption bands which could be ascribed to pyridinium species (formed upon adsorption on surface Brönsted acid sites) have been recorded, despite these sites having been detected using this same technique on Cr/TiO_2 solids where Cr was also in the 6+ state.[54] We may tentatively assume that a sort of cancellation might take place by the simultaneous presence of MgO in this solid.

When pyridine is adsorbed at room temperature on the sample calcined at 700 °C, the bands are recorded in the same positions, but they are weaker and disappear at 200 °C, a lower outgassing temperature than for the sample calcined at 500 °C, indicating that in this sample the surface Lewis acid sites are weaker, in agreement with previous studies. This difference cannot be originated by a change in the specific surface area, as coincident values have been measured for both samples, calcined at 500 and 700 °C (see Table 4), but to a decrease in Lewis surface acidity by the reduction of Cr^{6+} to Cr^{3+} species as the calcination temperature is further increased.

(54) Venezia, A. M.; Palmisano, L.; Schiavello, M.; Martín, C.; Rives, V. *J. Catal.* **1994**, *147*, 115.

Conclusions

Among the methods here used to prepare a Mg,Al hydrotalcite with intercalated $[Cr(C_2O_4)_3]^{3-}$, only ionic exchange has been successful, leading to a well crystallized hydrotalcite with a basal spacing of 10 Å. On the contrary, the reconstruction method did not lead to the desired product, probably because the high pH value due to the suspension of the MgAlC precursor calcined at 500 °C partially decomposes the chromium complex, with simultaneous partial dissolution of the hydrotalcite layers, leading to a polyphasic material, containing a layered material with intercalated complex units, amorphous magnesium oxalate, and small amounts of chromium oxohydroxides. Hydrothermal treatment further favors total decomposition of the complex, although the layered structure is respected with the same spacing, probably because some of the oxalate formed during decomposition of the complex is intercalated in an upward orientation.

The complex is stable in the interlayer up to 200 °C, although the free complex (as a potassium salt) decomposes at a higher temperature; chromate and oxalate species are formed above this temperature, the last one forming carbonate when the calcination temperature is further increased. The layered structure is destroyed at 340 °C, forming mostly amorphous phases and then crystallizing MgO.

Oxidaton of Cr^{3+} to Cr^{6+} takes place when calcination is carried out above 300 °C; this oxidation is complete at 400 °C, according to the TPR results, but reduction to Cr^{3+} species starts above 500 °C, finally forming a crystalline $MgAl_{1.5}Cr_{0.5}O_4$ phase.

The calcined materials exhibit larger specific surface areas than the original compound, and they exhibit only surface Lewis acid sites.

Acknowledgment. The authors acknowledge financial support from MCyT (Grant MAT2000-1148-C02-01), and Mr. A. Montero for recording the TPR analysis.

IC034034U